

## Hetero-assembly of gold nanoparticles on a DNA origami template

Jie Chao<sup>1,2†</sup>, Yinan Zhang<sup>2†</sup>, Dan Zhu<sup>1\*</sup>, Bing Liu<sup>2</sup>, Chengjun Cui<sup>2</sup>, Shao Su<sup>1</sup>,  
Chunhai Fan<sup>2\*</sup> & Lianhui Wang<sup>1\*</sup>

<sup>1</sup>Key Laboratory for Organic Electronics & Information Displays; Institute of Advanced Materials, National Synergetic Innovation Center for Advanced Materials, Nanjing University of Posts & Telecommunications, Nanjing 210023, China

<sup>2</sup>Division of Physical Biology and Bioimaging Center, Shanghai Synchrotron Radiation Facility; CAS Key Laboratory of Interfacial Physics and Technology; Shanghai Institute of Applied Physics, Chinese Academy of Sciences, Shanghai 201800, China

Received October 15, 2015; accepted November 10, 2015; published online April 15, 2016

Hetero-assembling of spherical building blocks with well-defined spatial distribution holds great significance in developing chiral nanostructures. Herein, a strategy for hetero-assembling of gold nanoparticles (AuNPs) was demonstrated using rigid bifacial DNA origami as templates. By tuning the sizes and the fixed location of AuNPs on DNA origami, right-handed and left-handed AuNPs nanostructures were respectively constructed. Gel electrophoresis indicated the formation of the DNA origami-AuNPs complex and transmission electron microscopy (TEM) visually displayed the arrangement of AuNPs in these two chiral structures. The spatial configuration and 3D geometry of AuNPs were further illustrated by the stereographic TEM with tilting angles from  $-30^\circ$  to  $30^\circ$ . This strategy provides a universal approach to construct the asymmetrical 3D geometries, which may have potential applications in biomimicking and nanophotonics.

**hetero-assembly, DNA origami, gold nanoparticles, chiral structure**

**Citation:** Chao J, Zhang YN, Zhu D, Liu B, Cui CJ, Su S, Fan CH, Wang LH. Hetero-assembly of gold nanoparticles on a DNA origami template. *Sci China Chem*, 2016, 59: 730–734, doi: 10.1007/s11426-016-5596-x

### 1 Introduction

Programmable assembly of nanoparticles into superstructures has attracted much attention in multidiscipline because of their potential applications in plasmonics and electronics [1,2]. Since the gold nanoparticles (AuNPs) own fascinating aspects such as multiple assembly types, high stability and size-related electronic, magnetic and optical properties (quantum size effect), it is an everlasting hot spot for research in this field [3]. DNA is introduced to assemble AuNPs by the famous covalent bond between gold and sulfur (Au–S) [4]. In the beginning, single-stranded (ss) or double-stranded (ds) DNA are used as linkers to assemble

AuNPs into nanostructures [5]. Elegant examples are the two independent pioneering pieces of work in Mirkin's and Alivisatos' group in the year of 1996 [6,7]. One of the challenges in this strategy was the rigidity of the ssDNA and dsDNA which limited the size of AuNPs for manipulation.

With the establishment of DNA as one type of highly precise and programmable materials for self-assembly, large numbers of DNA nanostructures have been fabricated in multiple dimensions [8–12]. These DNA nanostructures with well-defined geometry and topology open another door for the assembly of AuNPs, which can serve not only as linkers but as templates [13–17]. Especially with the birth of DNA origami technology which utilizes a long ss-DNA (viral M13mp18 of 7249 nucleotides) to fold with hundreds of short complementary staple strands [18], the forming predefined 2D and 3D nanostructures can serve as perfect templates for the assembly of AuNPs nanostructures with

<sup>†</sup>These authors contributed equally to this work

\*Corresponding authors (email: iamdzhu@njupt.edu.cn; fchh@sinap.ac.cn; lhwang@njupt.edu.cn)

rational morphology and symmetry [19–25]. Yan's group [26] first used the rectangle DNA origami template to organize AuNPs with two different sizes at predefined positions. Later, Ding *et al.* [27] assembled AuNPs with different sizes onto the triangular DNA origami to form a self-similar chain. Recently, researchers have more interests in the unique properties of AuNPs in plasmonics. Take circular dichroism (CD) responses for example, the natural chiral molecules including amino acids, peptide and DNA can only exhibit CD responses in the UV range, while artificial plasmonic structures own the special optical chirality which can reach into the visible and infrared ranges. In 2012, two groups separately demonstrated the chiral organizations of AuNPs on DNA origami template that both exhibited well-defined plasmonic CD responses and optical rotatory dispersion effects [28,29]. Their difference was that one employed a tubular origami as the template to organize the AuNPs into chiral nanostructures, the other rolled a square DNA origami with linear AuNPs into chiral nanostructures. Further, four identical gold nanoparticles were precisely organized onto the two faces of the rectangular DNA origami to generate a 3D asymmetric tetramer, which generated similar plasmonic CD effects [30]. Actually, it is very difficult to anchor AuNPs in larger sizes ( $\geq 30$  nm) onto a traditional DNA origami because of the charge repulsion. Here, we choose the hollow part of the triangular DNA origami to anchor the 50 nm AuNPs which can reduce the charge repulsion between DNA modified AuNPs and DNA origami. In addition, we also anchored another three AuNPs in different sizes onto the other face of the triangular DNA origami to make AuNP tetramers. Interestingly, these AuNP tetramers can be assembled into chiral nanostructures when the positions of two AuNPs were altered.

## 2 Experimental

### 2.1 Chemicals and reagents

All the chemicals were commercially obtained. The gold nanoparticles (10, 15, 20 and 50 nm) were purchased from British Biocell International (Cardiff, UK). M13mp18 single stranded DNA was purchased from New England Biolabs and was used as received. All the thiolated oligonucleotides of HPLC grade used were obtained from Takara Biotechnology and non-thiolated oligonucleotides of PAGE grade were from Sangon or Jie Li Biology. All water was purified with a Millipore Milli-Q® Integral water purification system (resistivity=18.2 M $\Omega$  cm).

### 2.2 Preparation of gold-DNA conjugates

AuNPs colloids were centrifuged at 8000 g for 10 min and the supernatant was removed by a pipette. The sediment was dispersed in ultrapure water. Thiolated oligonucleotides

S-T 30 were incubated with the Au NPs in a DNA to Au molar ratio of about 3000:1 in 0.5 $\times$ TBE buffer (89 mM Tris, 89 mM boric acid, 2 mM EDTA, pH 8.0) containing 50 mM NaCl for 2 h at room temperature. Then 2 M NaCl solution was slowly added to a final concentration of 0.5 M in another 3 h. After an overnight incubation, the excess DNA was washed out by centrifugation five times. The sediment was redispersed in 1 $\times$ TAE/Mg<sup>2+</sup> buffer (Tris, 40 mM; acetic acid, 20 mM; EDTA, 2 mM; and magnesium acetate, 12.5 mM; pH 8.0). The molar ratios of DNA/Au NPs were different for different sizes (5 nm: 100; 10 nm: 300; 15 nm: 800; 20 nm: 2000). The concentration of the Au NPs was estimated from the optical absorbance at  $\sim$ 520 nm.

### 2.3 Assembly of the DNA origami templates

The triangular DNA origami was prepared following a protocol by Rothemund. In a one-pot construction of triangular DNA origami template, 2 nM of M13mp18 DNA was mixed with 10 nM of staple strands which were annealed from 95 to 20 °C in a 1 $\times$ TAE/Mg<sup>2+</sup> buffer. The prepared DNA origami was then filtered with 100 kDa (MWCO) centrifuge filters four times to remove the extra strands. In a two-step assembly, the component strands were added to the prepared DNA origami followed by annealing from 45 to 30 °C and then cooling to 4 °C.

### 2.4 Assembly of AuNPs onto DNA origami template

The AuNPs were mixed with the triangular origami template at a molar ratio of  $\sim$ 2:1. The assembly was performed by annealing from 45 to 30 °C four times and then cooling to 4 °C. A 0.5% agarose gel electrophoresis (running buffer: 1 $\times$ TAE/Mg<sup>2+</sup>; loading buffer: 60% sucrose; 5 V/cm) was used to characterize the result of the assembly. The product was extracted from the gel with Freeze-Squeeze columns (Bio-Rad, USA) or dialysis tubing membranes.

### 2.5 TEM visualization of the AuNPs assemblies

The TEM samples were prepared by depositing 7  $\mu$ L of the sample solution on a carbon-coated TEM grid. After 10 min, the remaining solution was wicked from the grid using a pipette. Subsequently, a drop of water was deposited to remove the salt and then wicked by a pipette again. The grid was kept at room temperature to allow drying. TEM studies were conducted using a Tecnei G2-20S TWIN system (FEI, USA), operated at 200 kV in a bright field mode.

## 3 Results and discussion

### 3.1 Strategy for the hetero-assemblies of AuNPs on the DNA triangular origami

The coupling interactions between AuNPs have two effec-

tive coefficients, distance and size. DNA origami technology has supplied perfect platforms for the self-assembly of AuNPs because of their nano-scale resolution and hundreds of positions for immobilization of AuNPs which could precisely control the distance between AuNPs. But the large-sized AuNPs carrying more DNA strands seem to have much charge repulsion to the DNA templates which decreases the yield of their hybridization. To avoid such hindrance, the triangular DNA origami was selected as the template to anchor the 50 nm AuNPs whose hollow central part supplied more space for AuNPs to balance the charge repulsion. To facilitate the precise positioning of the AuNPs on the template, three staples on every inner edge of the triangular DNA origami template were prolonged with sequences complementary to the thiolated-DNA functionalized on the surface of the 50 nm AuNPs which may induce higher stability. The other three AuNPs with the size of 10, 15 and 20 nm were also assembled into the triangular DNA origami template by the same strategy (Figure 1). To decrease the steric hindrance between AuNPs, these AuNPs were anchored on the opposite face of the triangular DNA origami template. Interestingly, the position change of 10 and 15 nm AuNPs would generate two chiral nanostructures.

### 3.2 Characterization of chiral AuNPs nanostructures by gel electrophoresis

The AuNPs nanostructures products were analyzed by agarose gel electrophoresis. The resulting gel image is shown in Figure 2. The first four lanes from left to right respectively correspond to thiolated-DNA functionalized 15 nm AuNPs, 10 nm AuNPs, 20 nm AuNPs and 50 nm AuNPs, which are all as controls to direct the moving speeds. The last two lanes are the annealed product of the left- and right-handed nanostructures assembled on the triangular DNA origami template, respectively. Although bands of the byproducts including single AuNPs and other AuNPs assemblies are

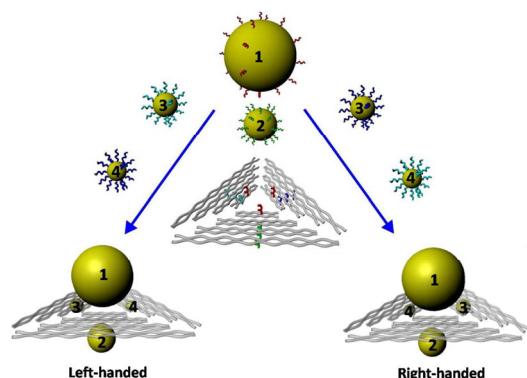


**Figure 1** Schematic showing of AuNPs assemblies on the DNA triangular origami into left-handed and right-handed nanostructures. AuNPs have four different sizes: (1) 50 nm; (2) 20 nm; (3) 15 nm; (4) 10 nm (color online).

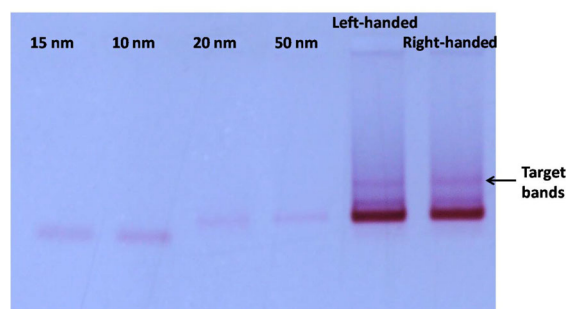


**Figure 2** Electrophoresis gel of chiral AuNPs assemblies. Lanes from left to right: thiolated-DNA functionalized 15 nm AuNPs, 10 nm AuNPs, 20 nm AuNPs, 50 nm AuNPs, left-handed AuNPs nanostructures, right-handed AuNPs nanostructures, in which the target bands are pointed out (color online).

still in these lanes, the target nanostructures are at the higher places which are highlighted with a black square. Two target AuNPs nanostructures were extracted from the gel bands with Freeze-Squeeze columns (Bio-Rad, USA).

### 3.3 TEM characterization of chiral AuNPs nanostructures

Transmission electron microscopy (TEM) allows us to view the AuNPs nanostructures directly. TEM images of the left-handed AuNPs nanostructures are shown in Figure 3. Although the samples are attracted from the target band in the gel, there still exist the AuNPs nanostructures with one or more small AuNPs loss which may be induced by inappropriate manipulation during the centrifugation or sample preparation. The zoom-in TEM images clearly demonstrate that the 50 nm AuNPs are embraced by three satellite AuNPs with the size of 15, 10 and 20 nm at different angles.

TEM images of the right-handed AuNPs nanostructures are shown in Figure 4. It also contains some other AuNPs nanostructures with one or more small AuNPs loss. The zoom-in TEM images clearly demonstrate the formation of

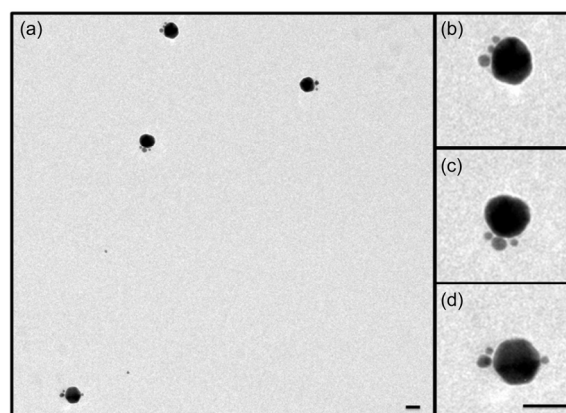


**Figure 3** Overview TEM images of left-handed AuNPs nanostructures (a) and zoom-in images (b-d). The scale bars are 50 nm.

50 nm AuNPs together with three other AuNPs at the size of 15, 10 and 20 nm around from different angles. Compared to Figure 3, three satellite AuNPs in Figure 4 seem larger. In fact, they are the same size while the 50 nm AuNPs used exhibit a little difference because they are in different production batches.

Furthermore, stereographic TEM imaging at different tilting angles was carried out to obtain more information about the 3D geometrical AuNPs nanostructures. The TEM images of left- (Figure 5(a–e)) and right-handed (Figure

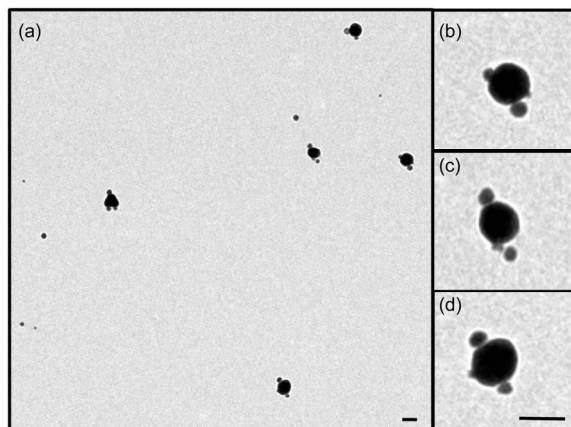


**Figure 4** Overview TEM images of right-handed AuNPs nanostructures (a) and zoom-in images (b–d). The scale bars are 50 nm.

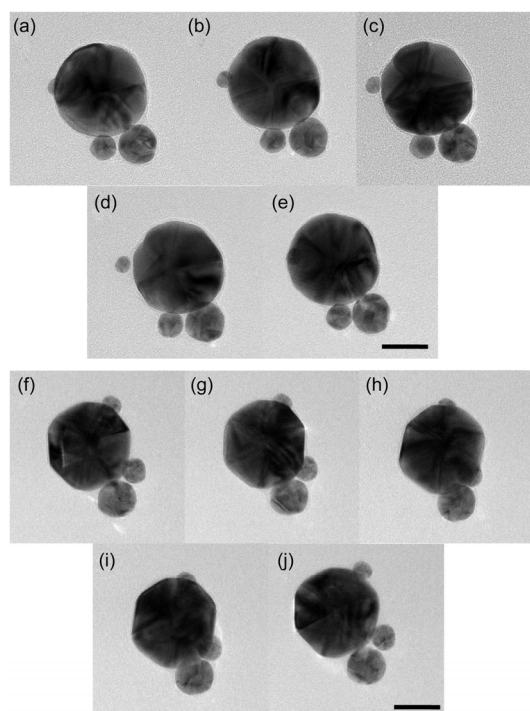


**Figure 5** (a–e) TEM images of an individual left-handed AuNPs nanostructure at tilting angle of  $-30^\circ$  (a),  $-15^\circ$  (b),  $0^\circ$  (c),  $15^\circ$  (d),  $30^\circ$  (e), respectively; (f–j) same for right-handed AuNPs nanostructure at tilting angle of  $-30^\circ$  (f),  $-15^\circ$  (g),  $0^\circ$  (h),  $15^\circ$  (i),  $30^\circ$  (j), respectively. The scale bars are 25 nm.

5(f–j)) structures are presented in Figure 5. The chiral characteristics of the nanostructures are directly shown in the images by changing the tilting angle from  $-30^\circ$  to  $30^\circ$ . Figure 5(c, h) shows the TEM images of left- and right-handed AuNP structures before tilting. After being tilted a certain angle, the change of relative position of the three small AuNPs (10, 15, 20 nm) distinctly demonstrated the 3D structure of these two hetero-assembled nanostructures.

## 4 Conclusions

In summary, we have successfully constructed AuNPs in varying sizes to form chiral nanostructures with nanometer precision by using DNA origami-directed self-assembly. Right- and left-handed nanostructures were fabricated by tuning the fixed position of AuNPs with certain sizes on the rigid addressable DNA origami. The spatial distribution and 3D geometry of the AuNPs nanostructures were visually displayed by stereographic TEM imaging at different tilting angles. This study has great significance in constructing nanostructures with some special optical properties because of the strong coupling interaction between metal nanoparticles. Furthermore, this approach may extend to the hetero-assembling of other nanoparticles (e.g., quantum dots, silver nanoparticles) with various sizes. By changing the morphology and shape of 2D DNA origami templates or using 3D DNA origami as templates, the spatial position of nanoparticles can be further regulated, which may have great potential in fabricating well-defined chiral nanostructures for versatile applications.

**Acknowledgments** This work was supported by the National Basic Research Program of China (2012CB933301), the National Natural Science Foundation of China (21305070, 21475064), the Natural Science Foundation of Jiangsu Province (BK20130861), the Sci-tech Support Plan of Jiangsu Province (BE2014719), and Science Foundation of Nanjing University of Posts and Telecommunications (213005, 214175).

**Conflict of interest** The authors declare that they have no conflict of interest.

**Supporting information** The supporting information is available online at chem.scichina.com and link.springer.com/journal/11426. The supporting materials are published as submitted, without typesetting or editing. The responsibility for scientific accuracy and content remains entirely with the authors.

- Henglein A. *Chem Rev*, 1989, 89: 1861–1873
- Alivisatos AP. *J Phys Chem*, 1996, 100: 13226–13239
- Daniel MC, Astruc D. *Chem Rev*, 2004, 104: 293–346
- Faltens MO, Shirley DA. *J Chem Phys*, 1970, 53: 4249–4264
- Loweth CJ, Caldwell WB, Peng X, Alivisatos AP, Schultz PG. *Angew Chem Int Ed*, 1999, 38: 1808–1812
- Mirkin CA, Letsinger RL, Mucic RC, Storhoff JJ. *Nature*, 1996, 382: 607–609
- Alivisatos AP, Johnsson KP, Peng X, Wilson TE, Loweth CJ, Bruchez MP, Schultz PG. *Nature*, 1996, 382: 609–611
- Kallenbach NR, Ma RI, Seeman NC. *Nature*, 1983, 305: 829–831

- 9 Winfree E, Liu FR, Wenzler LA, Seeman NC. *Nature*, 1998, 394: 539–544
- 10 Ding B, Sha R, Seeman NC. *J Am Chem Soc*, 2004, 126: 10230–10231
- 11 Wang YL, Mueller JE, Kemper B, Seeman NC. *Biochemistry*, 1991, 30: 5667–5674
- 12 Ma RI, Kallenbach NR, Sheardy RD, Petrillo ML, Seeman NC. *Nucleic Acids Res*, 1986, 14: 9745–9753
- 13 Xiao S, Liu F, Rosen A, Hainfeld J, Seeman N, Musier-Forsyth K, Kiehl R. *J Nanopart Res*, 2002, 4: 313–317
- 14 Pinto YY, Le JD, Seeman NC, Musier-Forsyth K, Taton TA, Kiehl RA. *Nano Lett*, 2005, 5: 2399–2402
- 15 Zheng J, Constantinou PE, Micheel C, Alivisatos AP, Kiehl RA, Seeman NC. *Nano Lett*, 2006, 6: 1502–1504
- 16 Claridge SA, Goh SL, Fréchet JM, Williams SC, Micheel CM, Alivisatos AP. *Chem Mater*, 2005, 17: 1628–1635
- 17 Sharma J, Chhabra R, Cheng A, Brownell J, Liu Y, Yan H. *Science*, 2009, 323: 112–116
- 18 Rothmund PWK. *Nature*, 2006, 440: 297–302
- 19 Douglas SM, Dietz H, Liedl T, Hogberg B, Graf F, Shih WM. *Nature*, 2009, 459: 414–418
- 20 Dietz H, Douglas SM, Shih WM. *Science*, 2009, 325: 725–730
- 21 Liedl T, Hogberg B, Tytell J, Ingber DE, Shih WM. *Nat Nano*, 2010, 5: 520–524
- 22 Han D, Pal S, Nangreave J, Deng Z, Liu Y, Yan H. *Science*, 2011, 332: 342–346
- 23 Wei B, Dai M, Yin P. *Nature*, 2012, 485: 623–626
- 24 Ke Y, Ong LL, Shih WM, Yin P. *Science*, 2012, 338: 1177–1183
- 25 Han D, Pal S, Yang Y, Jiang S, Nangreave J, Liu Y, Yan H. *Science*, 2013, 339: 1412–1415
- 26 Sharma J, Chhabra R, Andersen CS, Gothelf KV, Yan H, Liu Y. *J Am Chem Soc*, 2008, 130: 7820–7821
- 27 Ding B, Deng Z, Yan H, Cabrini S, Zuckermann RN, Bokor J. *J Am Chem Soc*, 2010, 132: 3248–3249
- 28 Shen X, Song C, Wang J, Shi D, Wang Z, Liu N, Ding B. *J Am Chem Soc*, 2012, 134: 146–149
- 29 Kuzyk A, Schreiber R, Fan Z, Pardatscher G, Roller EM, Hogele A, Simmel FC, Govorov AO, Liedl T. *Nature*, 2012, 483: 311–314
- 30 Shen X, Asenjo-Garcia A, Liu Q, Jiang Q, García De Abajo FJ, Liu N, Ding B. *Nano Lett*, 2013, 13: 2128–2133